

Large Eddy Simulation of Low Subcritical Reynolds Number Flow across a Rotating Circular Cylinder

K. MOBINI*

M. NIAZI

Department of Mechanical Engineering

Department of Mechanical Engineering

ShahidRajae Teacher Training University

ShahidRajae Teacher Training University

Lavizan, Tehran, 1678815811

Lavizan, Tehran, 1678815811

IRAN

IRAN

kmobini@srttu.edu

niazi400@yahoo.com

Abstract: - In this study, unsteady turbulent flow across a counterclockwise rotating circular cylinder is computed using Large Eddy Simulation (LES). The spin ratio varies between 0 and 2 and The Reynolds number changes from 3900 to 10000. Time integration of the flow equations is carried out for a very large dimensionless time. Smagorinsky subgrid scale model with $C_s=0.1$ is used to resolve the residual stresses. Variations of the mean drag and lift coefficients, and the flow structure with spin ratio and Reynolds number are studied. It is found that by increase of spin ratio or decrease of Reynolds number, both the stagnation point and the wake region move upward along the cylinder. As a result, the mean drag decreases and the mean lift increases. Length of the vortices behind the cylinder is also increased by increase of both spin ratio and Reynolds number. The computed results are compared with the results from the other numerical or experimental works, showing a good correspondence. It was found that the LES method is an accurate and convenient method for computation of highly recirculating flows.

Key-Words: - Large Eddy Simulation, Rotating circular cylinder, unsteady flow, drag coefficient, lift coefficient, subcritical flow

1 Introduction

Turbulent flow around bluff bodies, because of its vast range of applications and its complex physics, was the subject of many investigations for a very long time. There are various numerical methods and models to solve this problem. For example, Reynolds-averaged Navier-Stokes (RANS) method solves the problem using the time-averaged flow equations. This method can be accurate under certain conditions, but is not appropriate for transient and unstable flows. Direct numerical simulation (DNS) method directly solves all the small and large scales of turbulence without any modeling. It is the most complete turbulent model, but requires a huge amount of time and computational cost. Large Eddy Simulation (LES) directly solves the large scales (like the DNS

method), while it models the smaller scales (like the RANS methods). LES is more appropriate for such a problem, since it is more accurate than the RANS methods and less expensive than the DNS method. Flow around circular cylinders has had the highest number of investigations among bluff bodies. Many of these studies were performed on stationary cylinders at Reynolds number of 3900. Some of them, in which LES method is applied, are discussed here. Breuer [1] investigated the effect of grid size and subgrid scale on the drag and pressure coefficients using five networks with various grid numbers. He found out that the numerical dissipation produced by a scheme is more crucial for LES than its formal order of accuracy. Central schemes are better suited with LES than upwind schemes. He concluded that the dynamic

subgrid model combined with central differencing yields the best solution, which agrees quite well with experimental measurements. Blackburn and Schmidt [2] studied the two methods of spectral element large eddy simulation and finite volume large eddy simulation, and compared their results with the experimental results. They found out that the results from the spectral element method are more accurate. Franke and Frank [3] investigated the accuracy of the LES and compared the results with those from the DNS and experiments. They showed that the averaging time must be as large as possible, so that the mean values properly converge with good accuracy. Tremblay et al. [4] used both LES methods to solve the flow around a circular cylinder using Cartesian grids. They tested the influence of the subgrid scale model and the grid resolution. A fair agreement between LES and their previous DNS results was shown. Frohlich et al. [5] used LES method to solve the subcritical flow around circular cylinders using two methods: finite volume with structured grid and finite element with unstructured tetrahedral grid, and the results were compared together and with the other available results in the literature. They concluded that use of unstructured grid with sufficient accuracy requires a previous knowledge about the flow field, which is not really practical.

LES has also been applied to high Reynolds number flow across stationary cylinder. Breuer [6] applied LES to a challenging case of the Reynolds number of 140000. His aim was to evaluate the applicability of LES for practically relevant high-Reynolds-number flows and to examine the effect of subgrid scale modeling and grid resolution on the results. The results were in good agreement with experimental data. Catalano et al. [7] advanced further and applied LES to supercritical regime. They computed the flows with Reynolds numbers of 500000 and 1000000. The results were compared with the RANS results and some experimental results. LES results were found superior to the RANS results. Later, Yoshiyuki and Tetsuro [8] applied LES to critical and supercritical flow across a cylinder. They studied detailed structures of the separation bubble using time-sequential computed results as the Reynolds number changes.

In contrary to the case of stationary cylinder, comprehensive researches on the flow across rotating circular cylinder are more limited. The rate of rotational speed is usually expressed by spin ratio. Spin ratio is defined as the ratio of the cylinder's circumferential speed to the free stream speed. There are a number of studies on laminar flow past rotating cylinder, for which the

Reynolds numbers do not exceed 1000. Some of them are mentioned here. Badret al. [9] studied the unsteady flow across a rotating circular cylinder both numerically and experimentally at the Reynolds numbers from 1000 to 10000 and the spin ratios of 0.5 to 3. Their purpose was to investigate the effect of rotational speed on the flow structure. A good agreement between the two results were demonstrated. Stojkovic et al. [10] studied a new vortex shedding mode used on laminar flow across a rotating cylinder. It was found that the Strouhal number strongly depends on the spin ratio and weakly relates to the Reynolds number. Mittal and Kumar [11] analyzed the physics of the laminar flow passing a rotating cylinder at the Reynolds number of 200 and the spin ratios between 0 and 5. They found that vortex shedding stops at spin ratios greater than 1.91 and at the higher spin ratios the flow is stable. Padrino and Joseph [12] obtained the lift, drag and pressure coefficients at the Reynolds numbers of 200, 400 and 1000 while the spin ratio was changed between 3 and 6. They determined the position of the outer edge of the recirculating region as a function of the rotational speed.

There are a small number of studies on the flow across rotating cylinder with higher Reynolds numbers. Lam [13] has experimentally studied the flow around a rotating circular cylinder at Reynolds numbers between 3600 and 5000 and with spin ratios of 0 to 2.5, but he only investigated the vortex shedding behind the cylinder. Karabelas et al. [14] studied high Reynolds number turbulent flow past a rotating cylinder. They solved two-dimensional RANS equations via the finite-volume method closed by a modified $k-\epsilon$ turbulence model. The range of spin ratio was from 2 to 8 and Reynolds number changed between 5×10^5 and 5×10^6 . Elmiligui et al. [15] studied the flow past a rotating cylinder at the Reynolds number of 50000 and the spin ratios of 0 to 1. They used two multiscale type turbulence models based on modifying the RANS equations: a hybrid RANS/LES model and a modified version of the partially averaged Navier-Stokes (PANS) model. Aoki and Ito [16] studied a nonuniform flow across a rotating cylinder both experimentally and computationally at two Reynolds numbers of 60000 and 140000 and spin ratios between 0 and 1. Doll et al. [17] experimentally investigated the flow across a rotating cylinder at the Reynolds number of 9000 and the spin ratios from 0 to 2.7. They found out that the Strouhal number increases with spin ratio and vortex shedding stops at spin ratios greater than 2. Cheng et al. [18] solved the flow across a rotating cylinder at the Reynolds number of 6000

using discrete vortex method.

The only published work found by the authors on the use of LES for the flow across a rotating cylinder is the work of Karabelas [19]. He studied uniform flow past a rotating cylinder at $Re = 140,000$ with different spin ratios varying from 0 to 2.

The purpose of the current article is to apply LES to solve the flow past a rotating circular cylinder at the Reynolds numbers of 3900, 5000, 7000 and 10000 which are in the lower subcritical range. No published LES work on rotating cylinders in this range of Reynolds numbers was found by the authors. At the subcritical range of Reynolds numbers, the flow within the boundary layer on the cylinder surface is laminar up to the separation point, but after that the flow is turbulent and unstable. At each Reynolds number, the spin ratio is changed from 0 to 2. For each case, lift and drag coefficients are calculated and the streamlines are drawn. Some of the results are compared with the experimental and numerical results from other available researches.

2 Governing Equations

Governing equations are the incompressible continuity and Navier-Stokes equations, which are written as follows:

$$\frac{\partial u_i}{\partial x_i} = 0 \tag{1}$$

$$\frac{\partial u_i}{\partial t} + \frac{\partial(u_i u_j)}{\partial x_j} + \frac{1}{\rho} \frac{\partial p}{\partial x_i} = \frac{\partial(\nu 2S_{ij})}{\partial x_j} \tag{2}$$

In order to eliminate small scales, these equations are filtered using the filter convolution kernel G . \bar{u} is defined by:

$$\bar{u}(x) = \int_{-\infty}^{+\infty} G(x-x') u(x') dx' \tag{3}$$

\bar{u} is the filtered velocity and x' is dummy variable.

The filter length scale is denoted by Δ which is defined by:

$$\Delta = \sqrt{12 \int x^2 G(x) dx} \tag{4}$$

Applying the above filter on the governing equations, filtered continuity and Navier-Stokes equations are obtained as follows:

$$\frac{\partial \bar{u}}{\partial x_j} = 0 \tag{5}$$

$$\frac{\partial \bar{u}_i}{\partial t} + \frac{\partial(\bar{u}_i \bar{u}_j)}{\partial x_j} + \frac{1}{\rho} \frac{\partial \bar{P}}{\partial x_i} = \frac{\partial(\nu 2\bar{S}_{ij})}{\partial x_j} - \frac{\partial \tau_{ij}^r}{\partial x_j} \tag{6}$$

\bar{u}_i , \bar{u}_j and \bar{P} are the filtered velocities and filtered pressure respectively. τ_{ij}^r is the residual stress tensor and \bar{S}_{ij} is the filtered strain rate tensor defined by:

$$\bar{S}_{ij} = \frac{1}{2} \left(\frac{\partial \bar{u}_i}{\partial x_j} + \frac{\partial \bar{u}_j}{\partial x_i} \right) \tag{7}$$

To solve the small scale, Smagorinsky subgrid model [20] has been used. This model is based on eddy viscosity concept and relates residual stress tensor to filtered strain rate tensor by:

$$\tau_{ij}^a = \tau_{ij} - \frac{1}{3} \delta_{ij} \tau_{kk} = -2\nu_t \bar{S}_{ij} \tag{8}$$

Assuming that the small scales promptly dissipate all the energy received from the large scales, eddy viscosity is obtained from the following equation:

$$\nu_t = (f_\mu C_s \Delta)^2 |\bar{S}| \tag{9}$$

C_s is the Smagorinsky constant which is taken equal to 0.1. $|\bar{S}|$ is defined by:

$$|\bar{S}| = (2\bar{S}_{ij} \bar{S}_{ij})^{1/2} \tag{10}$$

The filter length is taken equal to grid size which is:

$$\Delta = (\Delta_x \Delta_y \Delta_z)^{1/3} = (\Delta V_{ijk})^{1/3} \tag{11}$$

f_μ is the Van Driest damping function which is used to damp turbulent fluctuations at the near wall regions.

Lift and drag forces are computed by carrying out integration on the cylinder surface area:

$$F_D = \int_s (\mu \frac{\partial v_t}{\partial n} n_x + P_{n_x}) ds \quad C_D = \frac{2F_D}{\rho U_\infty^2 dl} \tag{12}$$

$$F_L = \int_s (\mu \frac{\partial v_t}{\partial n} n_y + P_{n_y}) ds \quad C_L = \frac{2F_L}{\rho U_\infty^2 dl} \tag{13}$$

Here n_x and n_y are the Cartesian components of the unit vector n that is normal to the cylinder boundary. v_t is the component of velocity tangent to the cylinder surface.

Strouhal number is calculated from:

$$St = \frac{fD}{U_\infty} \quad (14)$$

f is the frequency of the vortex formation.

Spin ratio is calculated by:

$$\alpha = \frac{\omega \cdot D/2}{U_\infty} \quad (15)$$

ω is the angular velocity of the cylinder.

Reynolds number is defined by:

$$Re = \frac{\rho D U_\infty}{\mu} \quad (16)$$

3 Computational Grid and Numerical Method

To solve this problem a Ctype computational grid is used with dimensions of $l: 20D \times h: 10D \times w: \pi D$. Close to the counterclockwise rotating circular cylinder the grid is of Otype with diameter of $2D$. The cylinder is located at the distance of $5D$ from the entrance and it has the same distance from the upper and lower walls (Fig.1). Uniform velocity is used as the inlet boundary condition. At the outlet the fully developed boundary condition is considered. For the upper and lower walls, symmetry boundary condition is used and for the front and back walls, periodic boundary condition is chosen.

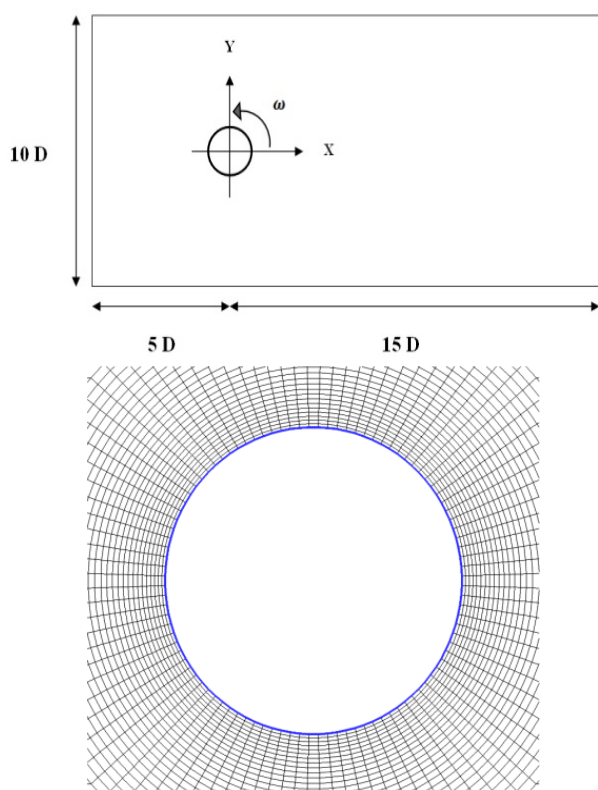


Fig.1. The computational domain and O grid around the cylinder.

Inlet velocity is taken as the initial condition throughout the entire computational field. Zero pressure is considered as the outlet boundary condition and as the initial condition through the entire field. Fine grid is used near the cylinder surface that requires a higher computational accuracy. As moving toward the walls the grid becomes coarser.

In this work, unsteady 3D incompressible Navier-Stokes equations have been solved for 60 seconds. Central difference method with second order accuracy is used for spatial and temporal discretization of the equations. The fully implicit finite volume method is applied. The time step for computation is considered as $0.07s$ and in each time step the Poisson equation is solved for pressure correction using the Simplec method. The Smagorinsky model with constant of 0.1 is used for subgrid scale modeling.

After using different grid sizes, a grid with 108800 cells was found to be the most appropriate one, and was used throughout the work.

4 Validation of the Computational Code

There are a number of experimental or numerical works performed on non-rotating cylinder at the Reynolds number of 3900. For the sake of comparison and validation of the current computational method, this Reynolds number has been used and the rotational speed is set equal to zero. The present results are compared with the experimental results of Norberg [21] and the numerical results of Breuer [1], Blackburn and Schmidt [2], Tremblay et al. [4] and Frohlich et al. [5]. Norberg [21] performed a number of experiments on a stationary cylinder at the Reynolds numbers of 50 to 40000, including 3900. The results are summarized in Table 1. It can be seen that the results of the current work are in a good agreement with both the experimental and DNS results, and this agreement is better than the other LES results.

Table 1. Comparison of the current work with experimental results and other numerical results.

	Method	SGS model	C_d	St
Norberg [21]	EXP	-	0.99	0.21
Tremblay et al. [4]	DNS	-	1.03	0.22

Blackburn and Schmidt [2]	LES	Smag. $C_s = 0.1$	1.07	0.24
Frohlich et al.[5]	LES	Smag. $C_s = 0.1$	1.08	0.21
Breuer B5 [1]	LES	Smag. $C_s = 0.1$	1.07	-
Present work	LES	Smag. $C_s = 0.1$	1.02	0.21

Fig.2 shows the variation of time-mean streamwise velocity along the horizontal line starting from the rear stagnation point $x/D=0.5$ through the wake down to $x/D=4.2$. Results from the present work have been compared with the experimental results of Lourenco and Shih [22]. The two results are in a very good correspondence from the cylinder end to $x/D=2$. Afterwards, there are discrepancies between the two curves which could be due to change of the grid type from O to C and changes in grid refinement. However, the two results are generally in an acceptable agreement.

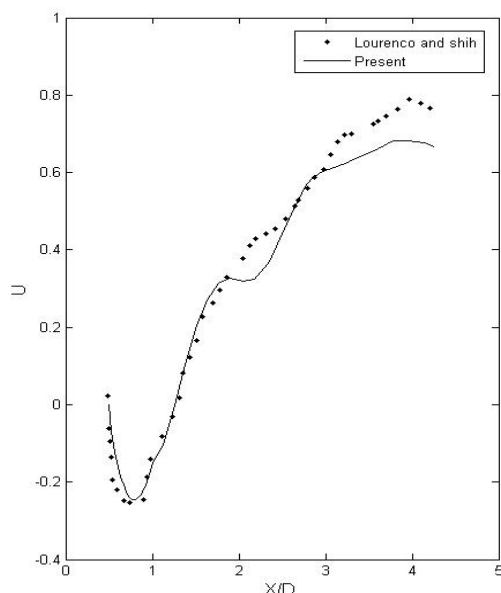


Fig.2. Time-mean streamwise velocity along the central line.

5 Results and Discussion

Physics of the turbulent flow past a rotating circular cylinder is different from that of a stationary cylinder. Rotation of the cylinder changes the flow speed around the cylinder and hence the whole flow field changes. In this work, five spin ratios of 0, 0.5, 1, 1.5 and 2 and four Reynolds numbers of 3900, 5000, 7000 and 10000 have been used.

In Fig.3 velocity contours around the cylinder for different Reynolds numbers and the spin ratio of zero are shown. In the spin ratio of zero (stationary cylinder) the passing flow velocities on the upper and the lower parts of the cylinder are approximately the same. The stagnation point is exactly located on the center line in front of the cylinder, and the separation points are symmetrical on the upper and lower surfaces. Von Karman vortices alternatively separate from the upper and lower surfaces for the first three Reynolds numbers, and they are symmetrical with respect to the central plane. Lengths of the vortices behind the cylinder are increasing by Reynolds number. For the Reynolds number of 10000, von Karman vortices disappear and a stretched symmetrical vortex area is observed behind the cylinder.

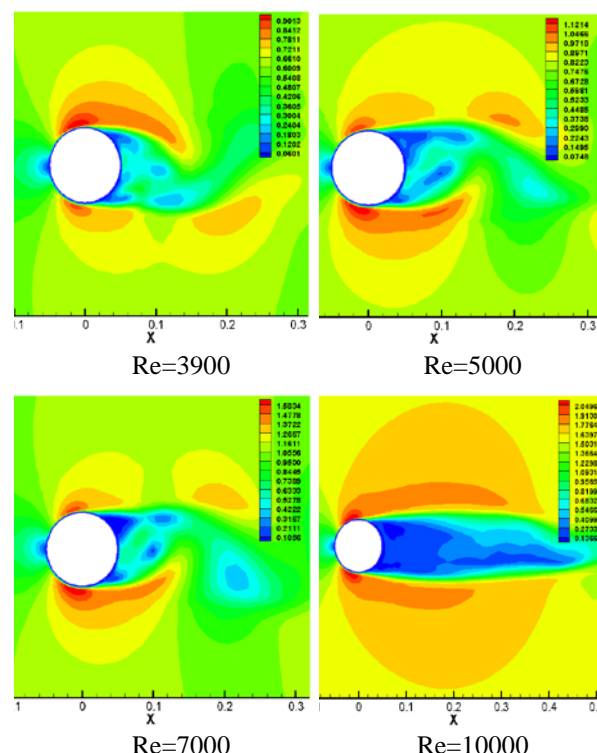


Fig.3. Velocity contours around the cylinder for the spin ratio of 0.

Flow pattern is completely different when the cylinder rotates. If the cylinder rotates counterclockwise, there will be a counter-current flow on the upper surface and a co-current flow on the lower surface. Therefore, flow velocity decreases on the upper surface and increases on the lower surface compared with stationary cylinder. Pressure has an opposite behavior on the two surfaces. A positive pressure increment on the top surface and an equal negative pressure

increment on the bottom surface create a negative lift force on the cylinder.

Fig.4 shows the velocity contours at the spin ratio of 0.5. It can be seen that the stagnation point is no longer on the center, and has slightly moved upward. The reason is that due to the counterclockwise flow on the cylinder surface, zero velocity occurs at a point located on top of the cylinder front center. Vortices behind the cylinder are no longer symmetrical and are slightly inclined upward. This is due to dislocation of the two separation points in the direction of the cylinder rotation. In other words, separation is advanced on the upper surface and is retarded on the lower surface. It can be seen that the upward inclination of the wake decreases by increase of Reynolds number, and the wake is more stretched.

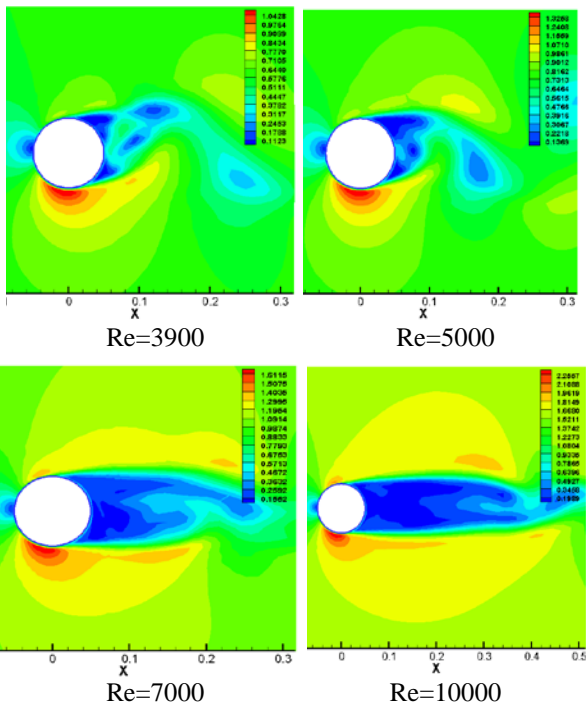


Fig.4. Velocity contours around the cylinder for the spin ratio of 0.5.

In Figs.5,6 and 7, the velocity contours around the cylinder for spin ratios of 1, 1.5 and 2 are plotted. It is observed that as the spin ratio increases, the upward dislocation of the stagnation point and the vortices behind the cylinder are increased. As a result, the stagnation point and the separation point on the upper surface get closer and closer.

Negative pressure increment on the lower surface and positive pressure increment on the upper surface are also increased by increase of spin ratio, resulting in increase of the downward lift.

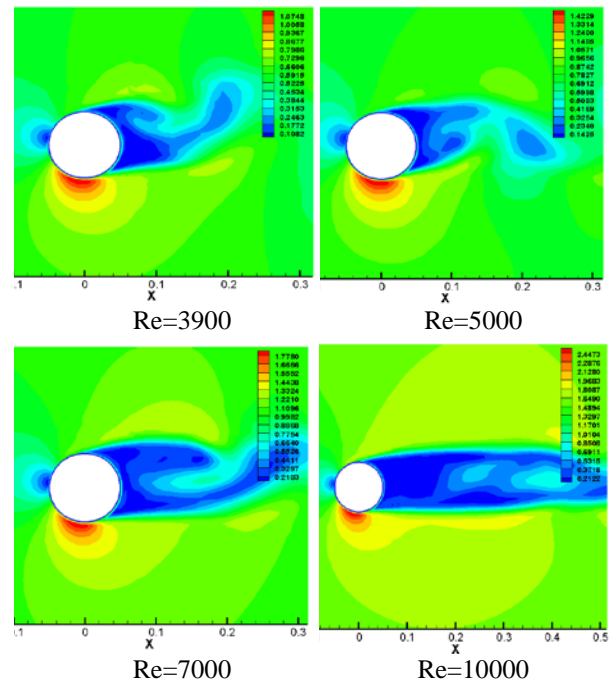


Fig.5. Velocity contours around the cylinder for the spin ratio of 1.

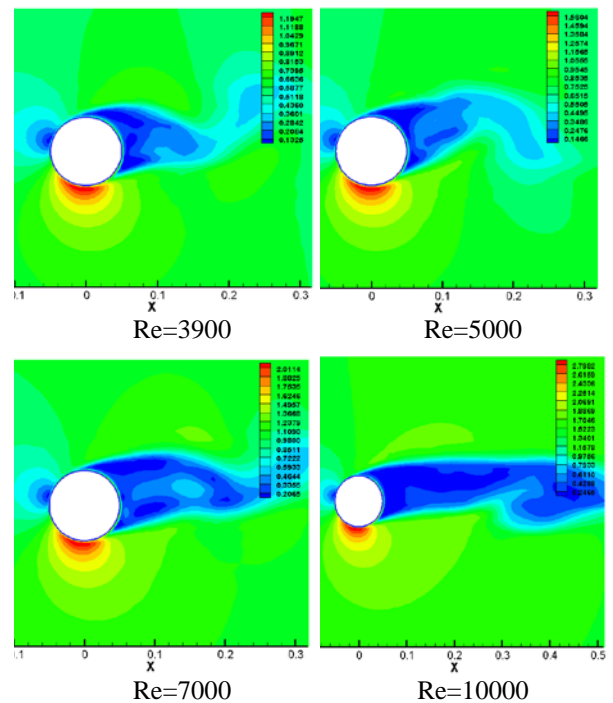


Fig.6. Velocity contours around the cylinder for the spin ratio of 1.5.

Another point to be noted is increase of the vortices length with increase of spin ratio while they become narrower and decline upward. This is due to upward displacement of the lower separation point and increase of the fluid velocity on the lower surface while at the upper surface it decreases.

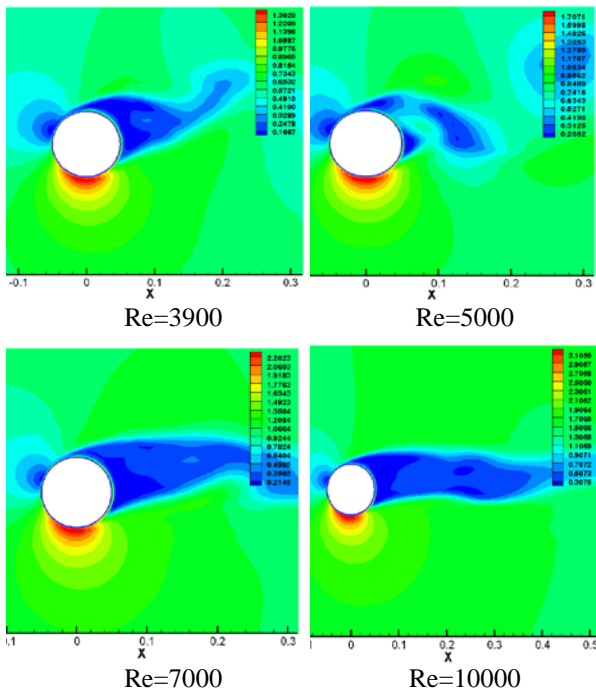


Fig.7. Velocity contours around the cylinder for the spin ratio of 2.

In Figs.8 and 9 drag and lift coefficients are plotted against spin ratio at different Reynolds numbers. Results from the present work are compared with the results of Kang et al [23] for the Reynolds numbers of 40 and 160 and Mittal and Kumar [11] for the Reynolds number of 200. Although the flows in these two works are laminar, comparison of the results shows the correct trend of the two aerodynamic coefficients.

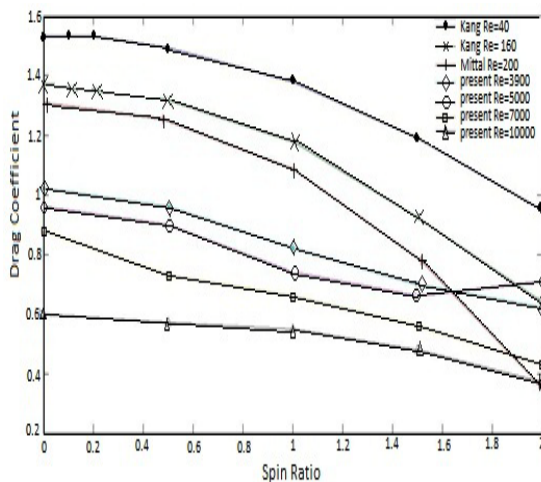


Fig.8. Drag coefficient versus spin ratio at different Reynolds numbers.

As seen in Fig.8, drag coefficient decreases with spin ratio. The reason for this reduction is the

upward dislocation of the stagnation point or the high pressure area. For stationary cylinder, the high pressure area is exactly located at the middle of the left semi-cylinder, and has the highest contribution to pressure drag. When this area moves upward, horizontal component of pressure on the left surface decreases, which leads to decrease of pressure drag.

Fig.8 also shows that drag coefficient decreases by increase of Reynolds number. Increase of Reynolds number is due to increase of free stream velocity. Increase of free stream velocity should be along with increase of the cylinder's angular velocity so that the spin ratio remains constant. Therefore, both rotational speed and Reynolds number are increased. The former tends to increase upward displacement of the stagnation point, while the latter has an adverse effect. Therefore, no change in the position of the stagnation point is expected when spin ratio remains constant. Hence, the reason for decrease of drag coefficient should be the changes in the wake area behind the cylinder. As seen in the velocity contour diagrams, the wake area behind the cylinder is more stretched and narrower when Reynolds number increases in a constant spin ratio. As a result, overall pressure on the right half of the cylinder increases, which leads to drag reduction. It can be seen in Fig.8 that there are some discrepancies in the normal trend at the spin ratio of 2 which must have a computational origin. The exact reason is still unknown to the authors.

According to Fig.9, lift coefficient increases with spin ratio. The reason is the upward displacement of the high pressure region with increase of angular velocity. This displacement increases the vertical component of the exerted force and hence the downward lift increases.

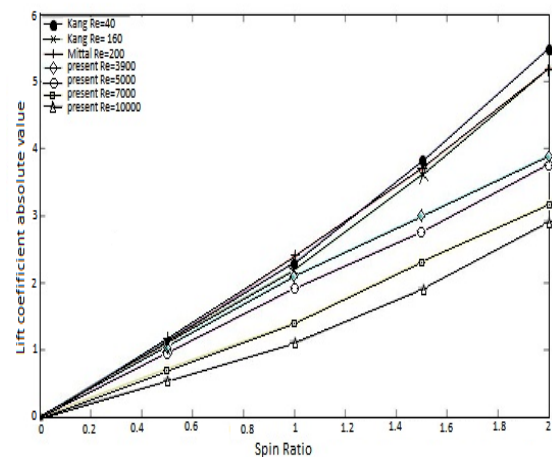


Fig.9. lift coefficient versus spin ratio at different Reynolds numbers.

It can be seen in Fig.9 that for the current work lift coefficient decreases with Reynolds number, whereas for the previous works there is no specific trend. Regarding the latter, the flow is laminar and the Reynolds numbers are very close. Therefore the curves are very close together, and any small source of computational error may cause the curves to intersect with each other. For the current work, lift force decreases with Reynolds number. This is due to decrease of the upward displacement of the wake with increase of Reynolds number. This means that separation point on the upper surface moves forward, which means higher velocity and lower pressure on the top. Lower top pressure means smaller downward lift force.

In Fig.10 variations of drag and lift coefficients with time are demonstrated for different spin ratios. For the stationary cylinder (spin ratio of 0), both the coefficients become almost statistically stationary after about 5 seconds. By increase of the rotational speed it can be seen that the time at which the coefficients become statistically stationary, increases. This is due to increase of instabilities by increase of the rotational speed which requires a longer time to reach stability.

For stationary cylinder, the averaged drag coefficient is about 1 and for the lift it is zero. By increase of the spin ratio, the averaged drag decreases and the absolute value of the averaged lift increases. This case was extensively discussed before.

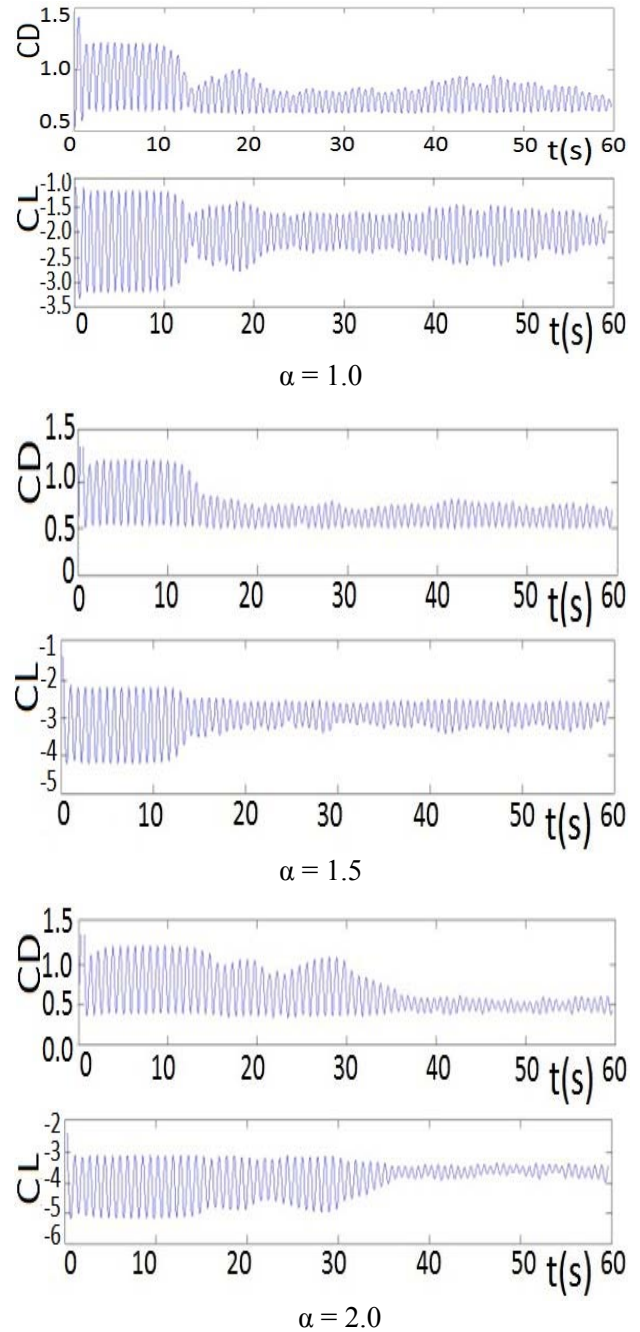
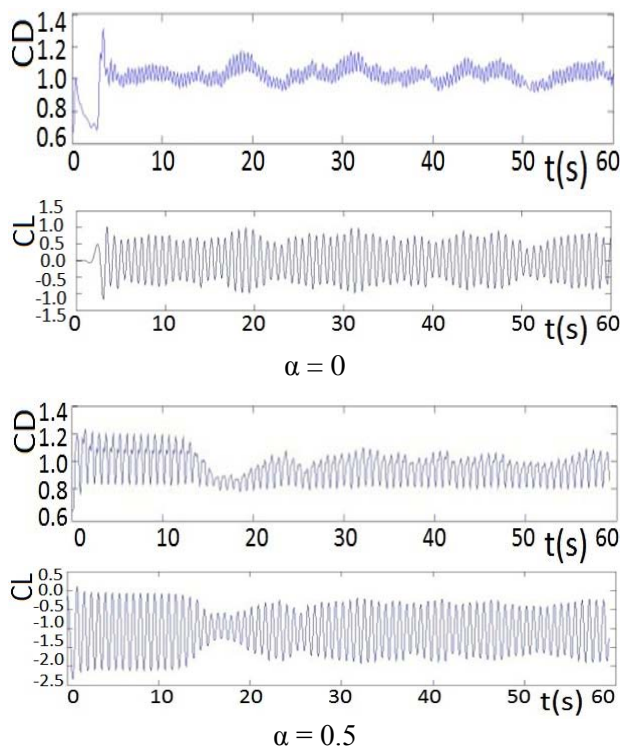


Fig.10. Drag and lift coefficients versus time for different spin ratios

At spin ratio of zero, amplitude of drag coefficient is very small (about 0.05) and for the lift it is much higher (about 0.7). This is due to the fact that the reason for the fluctuations is: intermittent grow and release of vortices on the upper and lower surfaces of the cylinder, and hence intermittent change of pressure on these surfaces. For stationary cylinder, vortex shedding from the upper and lower surfaces is symmetrical respect to the horizontal surface. Therefore, intermittent change of the horizontal forces on the upper and lower surfaces has only a minor effect on the total horizontal force

(drag). However, the change on the vertical forces and hence the lift is substantial.

This figure also shows that after reaching a stable condition, the amplitude of fluctuations decreases by increase of the spin ratio. This fact shows that the size and strength of the vortices decrease by the increase of spin ratio and vortex shedding eventually disappears.

6 Conclusion

Turbulent flow across a counterclockwise rotating circular cylinder is numerically studied using Large Eddy Simulation method with Smagorinsky subgrid scale model. Spin ratio has changed from 0 to 2 and Reynolds number has changed from 3900 to 10000. Comparison of the results with some other numerical and experimental results showed a good correspondence. According to the results, both the stagnation point and the wake region move upward and get close together by increasing the cylinder rotational speed. Therefore, the drag coefficient decreases and the downward lift coefficient increases. Increase of Reynolds number at constant rotational speed has an opposite effect on the stagnation point and the wake and reduces their upward displacement. It was also observed that the wake region behind the cylinder stretches by increase of both spin ratio and Reynolds number. The time required to reach a stable flow increases by increase of the rotational speed, while the amplitude of the fluctuations decreases by increase of the spin ratio.

It is found from this work that the LES method is capable of solving highly recirculating flows with great accuracy and with a low computational cost.

References:

- [1] Breuer, M., Large eddy simulation of the sub-critical flow past a circular cylinder: numerical and modeling aspects, *Int. J. Numerical Methods Fluids* Vol.28, 1998, pp.1281–1302.
- [2] Blackburn, H. M., Schmidt, S., Large Eddy Simulation of Flow Past a Circular Cylinder, *14th Australasian Fluid Mechanics Conference*, Adelaide University, Adelaide, Australia, 2001.
- [3] Franke, J., Frank, W., Large eddy simulation of the flow past a circular cylinder at $Re=3900$, *Journal of Wind Engineering and Industrial Aerodynamics*, vol.90, No.10, 2002, PP.1191–1206.
- [4] Tremblay, F., Manhart, M., Friedrich, R., LES of flow around a circular cylinder at a subcritical Reynolds number with cartesian grids, *Fluid Mechanics and its Applications*, Vol.65, 2004, pp.133–150.
- [5] Frohlich, J. Fr., Rodi, W., Kessler, Ph., Parpais, S., Bertoglio, J.P., Laurence, D., Large eddy simulation of flow around circular cylinders on structured and unstructured grids, *In: E.H. Hirschel (Ed.), Numerical flow simulation: CNRS DFG collaborative research programme*, Vol.66, Vieweg, Braunschweig, 1998, pp.319–338.
- [6] Breuer, M., A challenging test case for large eddy simulation: high Reynolds number circular cylinder flow, *International Journal of Heat and Fluid Flow*, Vol.21, 2000, pp.648–654.
- [7] Catalano, P., Wang, M., Iaccarino, G., Moin, P., Numerical simulation of the flow around a circular cylinder at high Reynolds numbers, *International Journal of Heat and Fluid Flow*, Vol.24, 2003, pp.463–469.
- [8] Yoshiyuki, O., Tetsuro, T., LES of flows around a circular cylinder at critical and supercritical Reynolds numbers, *American Physical Society, 61st Annual Meeting of the APS Division of Fluid Dynamics*, 2008.
- [9] Badr, H. M., Coutanceau, M., Dennis, S. C. R., Menard, C., Unsteady flow past a rotating cylinder at Reynolds numbers 10^3 and 10^4 , *J. Fluid Mech.*, Vol.220, 1990, pp.459–484.
- [10] Stojkovic, D., Schon, P., Breuer, M., Durst, F., On the new vortex shedding mode past a rotating circular cylinder, *Physics of Fluids*, Vol.15, No.5, 2003, pp.1257–1260.
- [11] Mittal, S., Kumar, B., Flow past a rotating cylinder, *J. Fluid Mech.* Vol.476, 2003, pp.303–334.
- [12] Padrino, J.C., Joseph, D.D., Numerical study of the steady-state uniform flow past a rotating cylinder, *J. Fluid Mech.* Vol.557, 2006, pp.191–223.
- [13] Lam, K. M., Vortex shedding flow behind a slowly rotating circular cylinder, *J. Fluids and Structures*, Vol.25, 2007, pp.245–262.
- [14] Karabelas, S.J., Koumroglou, B.C., Argyropoulos, C.D. and Markatos, N.C., High Reynolds number turbulent flow past a rotating cylinder, *Applied Mathematical Modelling*, Vol.36, No.1, 2012, pp.379–398.

- [15] Elmiligui, A., Abdol-Hamid, K. S., Massey, S. J. and Pao, S. P., Numerical Study of Flow Past a Circular Cylinder Using RANS, Hybrid URANS/LES and PANS Formulations, *AIAA*, 2004, Paper 2004-4959, 2004.
- [16] Aoki, K., Ito, T., Flow characteristics around a rotating cylinder, *In: Proceedings of the School of Engineering of Tokai University*, vol.26, 2001, pp.29–34.
- [17] Doll, S. S., Kopp, G. A., Martinuzzi, R. J., The suppression of periodic vortex shedding from a rotating circular cylinder, *J. Wind Engineering and Industrial Aerodynamics*, vol.96, No.6-7, 2008, pp.1164–1184.
- [18] Cheng, M., Chew, Y. T., Luo, S. C., Discrete vortex simulation of the separated flow around a rotating circular cylinder at high Reynolds number, *Finite Elements in Analysis and Design*, Vol.18, No.1–3, 1994, pp. 225-236.
- [19] Karabelas, S.J., Large Eddy Simulation of high-Reynolds number flow past a rotating cylinder, *International Journal of Heat and Fluid Flow*, Vol.31, No.4, 2010, pp.518-527.
- [20] Smagorinsky, J., General circulation experiments with the primitive equations. I. The basic experiment, *Monthly Weather Review*, Vol.91, No.3, 1963, pp.99–164.
- [21] Norberg, C., An Experimental Investigation of the Flow around a Circular Cylinder: Influence of Aspect Ratio, *J. Fluid Mech.*, Vol.258, 1994, pp.287-316.
- [22] Lourenco, L. M. and Shih, C., Characteristics of the Plane Turbulent near Wake of a Circular Cylinder; a Particle Image Velocimetry Study, (data taken from Beaudan&Moin 1994).
- [23] Kang, S., Choi, H., Lee, S., Laminar flow past a rotating circular cylinder, *Physics of Fluids*, Vol.11, 1999, pp.3312–3321.